Applied Ocean Research 150 (2024) 104141

Contents lists available at ScienceDirect

Applied Ocean Research

journal homepage: www.elsevier.com/locate/apor

Research paper

# On the experimental full scale vibrational response analysis of a large pleasure yacht

Paolo Silvestri [a], Tatiana Pais [b], Gianmarco Vergassola [b,*]

[a] Department of Mechanical, Energy, Management and Transportation Engineering (DIME), University of Genova, Italy
[b] Electrical, Department of Electronics and Telecommunication Engineering and Naval Architecture (DITEN), University of Genova, Italy

ARTICLE INFO

*Keywords:*
Experimental full scale vibration analysis
Yacht
Vibration
Spectral kurtosis

ABSTRACT

This paper presents an experimental investigation carried out on a large pleasure yacht during a sea trial using vibration signal processing methods to characterize its dynamic operational behaviour and to identify contributions of the main sources acting on the system including the onset of the propeller cavitation phenomenon.

Synchronous averages were computed to isolate vibration components associated with a specific source acting on the system. Their use jointly with variance computation allowed the detection of the rise of cavitation. Spectral Kurtosis analysis suggested optimal-bandwidth of the filter for system response demodulation and so better identify the rise of high frequency energy of bursting contents induced from cavitation strictly linked to propeller rotation.

Cyclic modulation spectrum was also adopted, which allows to extract the modulation features of cyclostationary signals, shows the rise of an interaction between high frequency contents and blade passage phenomenon approaching cavitating condition.

The results seem to provide an interesting solution based on the vessel vibrational response to define source contribution to the targets for a better identification of the dynamic system. Moreover, the proposed diagnostic methods reveal reliable tools for real time condition-based monitoring of the marine propeller to distinguish cavitation and wake energy contribution using vibrational response measured on the hull instead of hydrophone arrays.

## 1. Introduction

The hull dynamic excitations generated by propellers and propulsion diesel engines are significant vibration sources affecting dynamic operational behaviour of superyachts.

These dynamic sources located in the lower part of the hull, cause operational vibration levels that give rise to a continuous cyclic loading on the structures generating possible fatigue failure and a disturbance and reduction of health and comfort on the people on board, when the phenomenon is perceived as a deck vibration or a noise induced by vibration of ship interiors especially in presence of mechanical resonances (American Bureau of Shipping, 2006; Biot and De Lorenzo, 2007). Nowadays cruise companies of superyachts focus on the comfort for passengers who are always not accustomed to the marine environment and ensuring a comfortable trip has become a must to be competitive in the market (Asmussen et al., 2001; Lloyd's Register, 2006). To deep the dynamic operational behaviour has become more significant as undesirable vibrations and related vibroacoustic noise levels onboard can also be affected to the structural solution adopted for hull weight reduction, which leads to the design of increasingly lighter and inevitably more flexible structures, which therefore are more prone to amplify operational vibration responses. The noise and vibration reduction in ships is often achieved using viscoelastic materials coupled with the main steel structure (Silvestri et al., 2021). However, for an optimum dynamic operational behaviour aimed to reduce the vibrational response it is mandatory identifying vibration and noise sources contributions and main transfer energy paths the vessel and upper desks targets (Prato et al., 2023; Bassetti et al., 2022; Bassetti et al., 2022; Vergassola, 2019). On board sources also significantly contribute to the generation of underwater radiated noise that achieved great importance in the last years, because of the concerns about the consequence of acoustic pollution on marine ecosystems (Kalikatzarakis et al., 2022). The acoustic signature of a superyacht is typically dominated by machinery excitations until the Cavitation Inception Speed (CIS), i.e. the

* Corresponding author.
*E-mail address:* gianmarco.vergassola@unige.it (G. Vergassola).

https://doi.org/10.1016/j.apor.2024.104141
Received 2 April 2024; Received in revised form 19 July 2024; Accepted 21 July 2024
Available online 29 July 2024

vessel speed corresponding to propeller cavitation inception. Above this speed, cavitation noise dominates most of the radiated noise operational spectrum. Due to this, when more stringent noise requirements have to be met, it is usually necessary to operate the ship below its inception speed. Accurate prediction of the cavitation of a full-scale propeller cannot be achieved at present, so that only the real-time condition monitoring method can be used to obtain the cavitation state of a propeller during navigation. Cavitation detection is usually carried out analysing signals from sensors installed on board the ship. In principle, sensors, pressure transducers and accelerometers can be used for these purposes, however, from a practical point of view accelerometers are preferred because of their simpler and non-intrusive installation (Aktas et al., 2016). Cavitation presence can be assessed analysing the energy content of the signal, possibly focusing the analysis on relevant frequency bands. Accordingly, cavitation detection criteria can be defined as the signal energy exceeding a given threshold. Although this principle can be very effective it relies heavily on the threshold definition and it can cause false positive when other noise sources with varying intensity are present (Borelli et al., 2021). Alternatively, cavitation can be detected by verifying the presence into acquired structural signals of some specific characteristics related to the cavitation phenomenon. In some cases, propeller cavitation onset is identified by propeller inflow characteristics modification, i.e. the hull wake, causing cavitation bursting broad band noise to be periodic. This specific characteristic is exploited by the approach proposed in (Lee and Seo, 2013), based on Detection of Envelope Modulation On Noise (DEMON) analysis.

In the present work, system operational response has been investigated in a wide operating range conditions also including the ones characterized by cavitation and wake phenomena in order to obtain a complete dynamic characterization of the investigated vessel. Vibrational measurements allowed to identify the dominant spectral contents in system responses and to associate them the likely related sources. Then different methods of signal processing analysis were applied to the vibrational response signals to identify incipient propeller cavitation conditions and find reliable condition monitoring solutions to correctly detect this phenomenon to be avoided.

The main goal is to obtain a suitable method capable to reliably detect cavitation inception by relying only on vibrational system response to use cheap not intrusive vibrational sensors, instead of expensive and complex measurement campaign with hydrophones arrays. The diagnostic capacity of these sensors was found to be reliable despite background noise limiting signal-to-noise ratio at low frequency values and the presence of the hull structure that acts as a filter altering the cavitation energy content detectable on the measured vibrational system responses.

A method for detecting cavitation occurrence based on the spectral variance function evaluated on synchronous average vibration spectra is firstly considered (Combet and Gelman, 2007; Oppenheim and Schafer, 1999). This approach appears to be a valuable tool for identifying the rise of anomalous propeller conditions caused by random phenomena as soon as cavitation occurs.

In addition, cavitation has been detected by verifying the presence into acquired structural response of some specific characteristics related to triggering cavitation energy emission. In most cases, propeller cavitation onset and size are triggered by the characteristics of the propeller inflow causing cavitation bursting noise to be periodic. This feature is exploited by the approach proposed in (Borelli et al., 2021), based on envelope spectrum analysis of the filtered response signal. The approach presented in these works takes also advantage of the use of Spectral Kurtosis (SK) (Borelli et al., 2021; Lee and Seo, 2013; Combet and Gelman, 2007) to perform an optimized demodulation of the accelerometer signals to extract the contents of interest related to cavitation also in presence of significant noise levels.

Finally, an analysis of the cyclostationarity of the signal contents was conducted to underline how moving towards cavitation conditions, some components present in the acquired structural responses excited by cavitation phenomenon rise and are markedly affected the blade passage phenomenon.

**Fig. 1.** Resilient mounts used to uncouple the diesel engine from the ship hull, with a mono-axial accelerometer used to measure the vertical vibration levels at the diesel foundation.

To achieve this objective, an extensive experimental activity was carried out in a sea trial during a performance qualification test which allows to collect a wide data set useful foe the subsequent analysis.

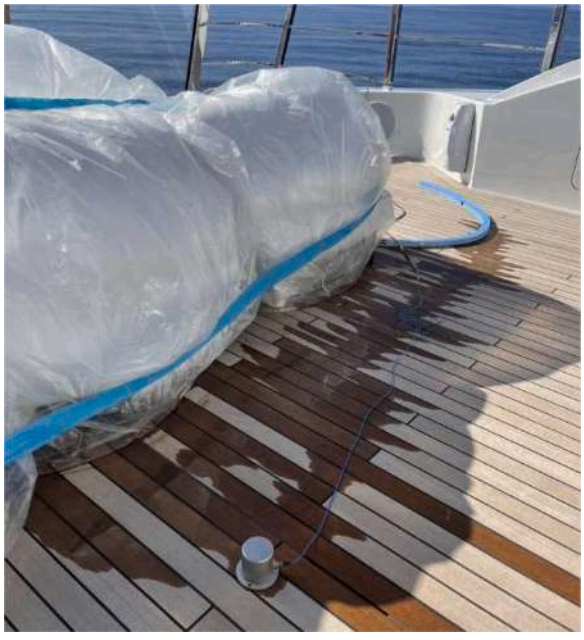

**Fig. 2.** Mono-axial high sensitivity accelerometer used to measure the vertical vibration levels at the sun deck.

## 2. Study case description

The investigation was carried on a 52-metre superyacht equipped with a traditional propeller propulsion system, featuring two five-bladed propellers connected to two 12-cylinder V 60° configuration 4-stroke marine diesel engines through a gearbox with a reduction ratio of 4.033.

Operational measurements were performed during a sea trial to evaluate on-board vibration levels.

The data were acquired in time domain using IEPE accelerometers, which were calibrated before and after the measurement survey. The analogue data from the sensors were converted into digital signals using a 16CHs Siemens LMS Scadas portable data acquisition system. The adopted sample rate was 4096 Hz. Although the adopted sampling frequency does not fully capture propeller operational high-frequency phenomena, it seems suitable for collecting a significant amount of energy content related to cavitation phenomena in the acquired responses as it allows to correctly measure higher orders of the blade passage phenomenon where the energy of the peak of tip vortex cavitation is significant (Kalikatzarakis et al., 2022; Aktas et al., 2016). This suitability is further confirmed by a vibration response time-frequency analysis during a propeller run-up test reported hereafter, which revealed that above a threshold rotation speed, specific contents attributable to structural resonances excited by broadband energy that may be related to cavitation are accurately measured.

Vibrational signals were collected by exploiting mono-axial accelerometers placed on the hull and on the decks (Figs. 1 and 2). For vibration response measurements near on structural girders, beams and hull shells standard sensitivity 100 mV/g accelerometers have been used (PCB Model 333B32) while high sensitivity ones (1000 mV/g) for target measurements on decks (PCB Model 393C). Two low sensitivity 10 mV/g accelerometers for engine block radial vibration component' measurements (PCB Model 353B03 with a measurement Range equal ±500 g peak) were adopted. All the adopted vibrational sensors were characterized by good dynamic response in the investigated frequency range.

Employed standard and low sensitivity accelerometers have an error of ± 5 % in the range 5Hz-5 kHz, while high sensitivity ones the same error in the range 2Hz-1 kHz. All types of accelerometers are characterized by a broadband resolution minus than 0.0002 g rms (0.000005 g rms for high sensitivity ones).

A sound pressure signal was also acquired by exploiting a prepolarized microphone with linear frequency response in the frequency range 2–25 kHz (measurement uncertainty of ± 2 dB, from 3.15 Hz to 25 kHz) and 22 dB(A) inherent noise (re=20μPa). This microphone was placed in correspondence of the swimming pool. The goal was to correctly investigate perturbation propagation phenomena from sources to targets during operational sea trials test. A one pulse per revolution trigger signal obtained from an optical high-speed probe has been acquired to evaluate propeller shaft rotation and obtain a phase reference for harmonic analysis. Standard data processing has been performed in Siemens Simcenter Testlab software, a commercial platform for sound and vibration analysis.

The surveys were carried out at different vessel cruising constant speed conditions (ranging from 4kn to 20kn) corresponding to propeller rotational velocity from 268 rpm to 434 rpm.

Measurements were performed while the sea state was 1 to avoid the influence of the ship motions on the measured data. A vibration measurement has been done with an accelerometer positioned on the hull shell immediately above a propeller to evaluate the dynamic response by the propeller-induced hull pressure pulses. A vibration response was acquired at the diesel foundations in correspondence of one of the resilient mounts, which were used to decouple the diesel engines from the ship structures to characterized propulsion engine excitation. The forced vibration responses induced by on board sources were measured also on targets defined on some accommodation decks.

All measurements were sampled continuously in specific time acquisition runs whose duration is ranging from 120 s to 600 s on the basis of the specific operational condition to be captured.

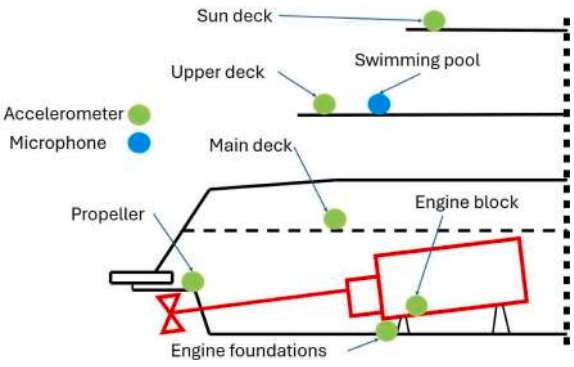


**Fig. 3.** Positioning scheme of the mono axial accelerometers and the microphone.

In Fig. 3 the positioning of the adopted mono axial accelerometers and 1 microphone is shown.

## 3. Processing techniques on operational sea trials response signals

Once the measurement surveys were completed, a signature analysis was performed on acquired data and averaging techniques have been adopted for source contribution analysis at the targets. In addition, processing techniques were performed on the measured data sets acquired during the sea trials to assess their reliability in correctly predicting propeller cavitation onset.

### 3.1. Operational signature analysis and spectral variance computation

Vibration analysis was initially applied to the acquired data to examine the dynamic structural characteristics of the system in operation condition and obtain its vibration signature in the frequency domain. Synchronous averaging (SA) technique was adopted that allows to extract periodic waveforms from noisy data applied both with linear and energy option on the operational vibrational responses. For this aim, a signal phased-locked with the angular position of the propeller shaft was acquired using an optical sensor, where the time at which the tachometer signal crosses from low to high is called the zero crossing corresponding to a reference angular position on the propeller shaft. Diesel trigger signal was obtained positioning an accelerometer on the engine block. Its signal was properly band-pass filtered around the crankshaft synchronous frequency to identify engine periodicity for subsequent synchronous analysis.

Linear synchronous averages allow to put in evidence harmonic deterministic contributions related to the reference considered periodic phenomenon (propeller rotation or diesel engine cycle) and reduce frequency contents energy due to both random phenomena and not-synchronous ones. Vice versa, energy synchronous ones better underline the contributions due to random phenomena on the deterministic one. As they are not conditioned by the phase value, results are the same if computed on data referenced to engine or propeller trigger (Combet and Gelman, 2007; Oppenheim and Schafer, 1999).

The spectral variance, using operational spectra as a statistical input data set, has been computed for cavitation detection purpose according to (1):

$$\sigma(\omega_k)^2 = (1/n)\sum\left(x(\omega_k)_i - x(\omega_k)_{\text{average}}\right)^2 \quad (1)$$

It is a frequency function based on second-order statistic that puts in evidence about cyclic variability and random content in conjunction with frequency. The amount of variance per k frequency component is the information returned by the obtained spectral function. This tool

allows for the detection of an increase in the lack of stationarity in a phenomenon characterized by specific frequency content. In the following, this method is applied for diagnostic purpose considering the frequency contents related to propeller rotation and blade passage phenomena sensitive to the approach of propeller cavitation conditions and the rise of bubble cavitation.

### 3.2. Spectral kurtosis tool for propeller cavitation identification

Spectral kurtosis (SK) is a statistical tool based on the moment of order 4 that exhibits low values when data is stationary and Gaussian and high values when transients occur. Spectral kurtosis may be used to detect faults and degradation that give rise to higher levels of response impulsivity and increasing of nonstationary and non-Gaussian system behaviour.

SK is defined as the energy normalized fourth-order spectral cumulant. An estimator can be computed from the short time Fourier transform (STFT) $|X(t,f)|$ of a signal x(t) according to (2):

$$\mathrm{SK(f)} = \frac{\left\langle |X(t,f)|^4 \right\rangle}{\left\langle |X(t,f)|^2 \right\rangle^2} - 2 \tag{2}$$

where $\langle \bullet \rangle$ denotes the time averaging operator. SK frequency resolution directly is related to the currently adopted window length in the STFT computation (Antoni, 2006).

It is fine for identifying incipient fault operating conditions as it is a statistical indicator and, as such, is generally more sensitive to the rise of anomalous trends in the system's dynamic response, even in conditions where high levels of noise could significantly hide the contents of interest.

The SK offers a specific approach to define optimal filters for extracting the mechanical signature of faults. It allows to identify the best compromise between a filter bandwidth that is too wide, which would alter the signal-to-noise ratio, and one that is too narrow, which would modify the nature of the anomalous content in the system dynamic response (Antoni, 2006). This is achieved through the introduction of the concept of a kurtogram, from which the optimal filtering parameters can be deduced. The kurtogram applies SK locally in different frequency bands, allowing it to analyse the entire frequency domain and identify those frequency ranges where the fault signal can be best detected. The diagnostic method is subsequently supported by envelope analysis for signal demodulation (Antoni, 2006).

In literature there are many effective diagnostic applications for the detection of tooth cracks in gears and rolling bearing faults (Antoni and Randall, 2006). In addition, for real time diagnostic applications of the method, the fast kurtogram algorithm is available which uses bandpass filtering along with a simplified computation to approximate the spectral kurtosis for each window size and frequency value (Antoni and Randall, 2006).

The paper evaluates the applicability of SK to detect the incipient propeller cavitation phenomenon onset when approaching a high-speed cruise condition. In (Lee and Seo, 2013) the authors have already experimentally investigated SK method computed on hydrophone signals for the detection of tip vortex cavitation in propeller from a complete model ship mounted in the water cavitation tunnel.

In the present activity SK diagnostic capability in cavitation detection is verified using structural vibration responses acquired during a sea trial. In this case its identification seems to be critical since analyses are performed on accelerometer signals whose energy also depends on structure dynamic characteristics, which acts like a high-pass frequency filter. Consequently, it may significantly alter frequency energy contents related to fluid-dynamic cavitation dynamic loads making difficult the detection of this phenomenon. Moreover, the vibration signals can be significantly contaminated by other noise sources except the cavitation making the detection more difficult. Despite these conditions, the SK has been revealed to be an effective and reliable tool for evaluating specific contents in the structural response related to the onset of cavitation.

Propeller shaft rotation interacts with cavitation phenomenon, inducing to a modification of the dynamic system response. In this condition, anomalous blade load distributions are characterized by impulsive phenomena and random fluctuations with periodically modulated broadbands energy by the propeller rotation. The consequent anomalous dynamic loads may excite system resonances giving rise up of new contributions and modifying the forced response.

Classical signal processing techniques may not be appropriate for detection of these phenomena, especially in an incipient condition as measured vibrational response signals are often heavily affected by significant background noise, may hide all other contents of diagnostic interest.

SK reveals to be able to detect in the cavitation condition the presence of a modulation behaviour in the system's dynamic responses allowing for the precise identification of the propeller shaft frequency as the characteristic frequency involved and specific system structural resonances as the modulated response contents. To get this, firstly the envelope of the properly band-pass filtered vibrational signal is computed; then the subsequent envelope spectral analysis would provide low frequency contents, i.e., the repeating propeller frequency and its higher multipliers. This put in evidence how cavitation of propeller is associated to a bursting excitation due to the tip vortex repeated in a periodic manner related to shaft rotation. SK appears to be suitable for this situation, as it can improve the demodulation process to effectively detect the rise of impulsiveness and modification of the system response contents also in the presence of strong additive noise.

### 3.3. Cyclostationarity analysis method for propeller cavitation identification

Cyclostationarity signal is defined as a signal that undergoes periodic modulations whilst regarded as non-stationary on a long-term basis (Antoni, 2009). Cyclostationary analysis can provide a powerful tool, which is more efficient than those of traditional spectral analysis with respect to the exhibition and verification of the various physical modulation mechanisms present system dynamic response.

In this context, such kind of analysis is exploited to assess cavitation condition, in order to look for energy periodicities conveyed by the acquired signal system responses which may be covered by deterministic and non-deterministic components and so not easily identifiable in the conventional spectrum. Cyclic spectral density function is the double Fourier transform of the covariance function and allows to analyse cyclostationary signals identifying all modulating cyclic frequencies α in all signal frequencies f. It is a two-dimensional function in the bi-frequency plane frequency $f$ and cyclic frequency α and provides an indication of the average amount of correlation between the signal frequency components at frequencies $f \pm \alpha$ (Antoni, 2009). When it is read along the α-axis, it presents the modulations and the hidden periodicities in signal energy in the form of a power spectrum. When cyclic spectral density function map is read along the f-axis, it shows, like in a PSD, the frequency contents and/or the random nature of a signal.

Cyclic spectral density (CSD) function is defined according to (3):

$$CSD_x^{\alpha}(f) = \lim_{\Delta f \to 0} \lim_{T \to \infty} \frac{1}{T\Delta f} \int_T x_{\Delta f}(t; f + \alpha/2) \cdot \overline{x_{\Delta f}(t; f - \alpha/2)}\, e^{-j2\pi\alpha t} dt \tag{3}$$

where $\overline{\bullet}$ denotes complex conjugate operator and Δf the bandwidth of the filter applied on the signal at the frequency $f+\alpha/2$ and f-α/2 (Antoni, 2009).

Since modulated signals exhibit cyclostationary behaviour, cyclic spectral density can be used to recognize cyclostationary modulated signal in a background of stationary noise as it is an energy density that shows which energy spectrum frequencies $f$ are modulated by some others α (Antoni and Hanson, 2012).

Cavitation generates collapse of air and vapour bubbles due to the passage of the propeller blades through the water and this action, cyclic in nature causes amplitude modulation in the generated excitation and as a consequence an amplitude modulation content in the measured system response (Kalikatzarakis et al., 2022; Aktas et al., 2016). The modulation of the shaft rotational frequency is due to the slight physical differences between blades, that causes one blades to cavitate more than the others. In these conditions, the forced response related to this propeller excitation is characterized by periodic variance which is correlated with periodically modulated broadband contribution of the cavitation phenomenon. The system response is classified as a second-order cyclostationarity signal as its periodic variance (Antoni, 2009). Cyclostationarity properties have been exploited in the early identification of propeller cavitation phenomenon as it has the advantage of using a more realistic model for the signal than the ones used in most of the conventional signal processing techniques jointly the high capability in weak-signal detection also in severe noise and interference environments.

## 4. Results and discussion

The results obtained by means of the previously described signal processing techniques are discussed in detail hereinafter.

### 4.1. Synchronous averages results

Accelerometer signals were firstly analysed to characterize system dynamic behaviour in terms of vibrational signature. Synchronous averages were evaluated in angle domain with reference to an integer number of propeller rotations or engine crankshaft rotations in a steady operation condition of the boat characterized by constant propeller rotational speed. The acquired uniform Δt signals were resampled at constant increments of shaft angle in order to obtain synchronously sampled data to use order tracking analysis (Fyfe and Munck, 1997). Synchronous sampling uses a revolution basis that produces an order spectrum.

FFT analysis has been employed to observe how the frequency contents in the acquired signals change at different rotational speed levels. SA spectra were computed both for propeller and engine sources on 100 extracts and this number of samples was found to be suitable to correctly remove all non-deterministic part of the signal and keep periodic components (Braun, 2011; McFadden and Toozhy, 2000).

Although the propeller and diesel are not independent rotating sources due to the presence of a kinematic coupling imposed by match of the mechanical transmission, it was still possible to separate the contributions of each of them in the measured responses adopting synchronous averages method.

This has been possible as in this case the transmission ratio (defined as the rotational speed ratio of the two sources) is not an exact integer rational number (4.033). Its value very close to an integer made it possible to define a significant number of phased time history extracts with reference to one of the two sources (propeller or engine cycle) which at the same time are not phased with reference to the cyclicity of the other source. The averaging process, applied on an adequate number of samples, allowed to obtain dynamic response spectra with separate contents for the diesel and propeller sources in the frequency range of interest.

Fig. 4 reports synchronously linear averaged complex spectra triggered both on propeller rotation (top) and diesel engine cycle (bottom) of the vibration signal measured in correspondence of one of the resilient mounts at propeller shaft 416 rpm. In addition, energy averaged complex spectrum is also reported. Energy averaged process doesn't take into account the phase and the obtained spectra are the same for both references (except for small differences related to the averaging process).

On all the graphs, as the computed spectral lines are a fixed order distance, the primary x axis is the order one. In addition, a secondary x axis at the top has been inserted that reports the corresponding derived frequency.

Linear synchronously averaged spectrum with reference to the rotation of the diesel engine indicates that are well detectable characteristic engine frequency contents related to engine cycle (0.5X),

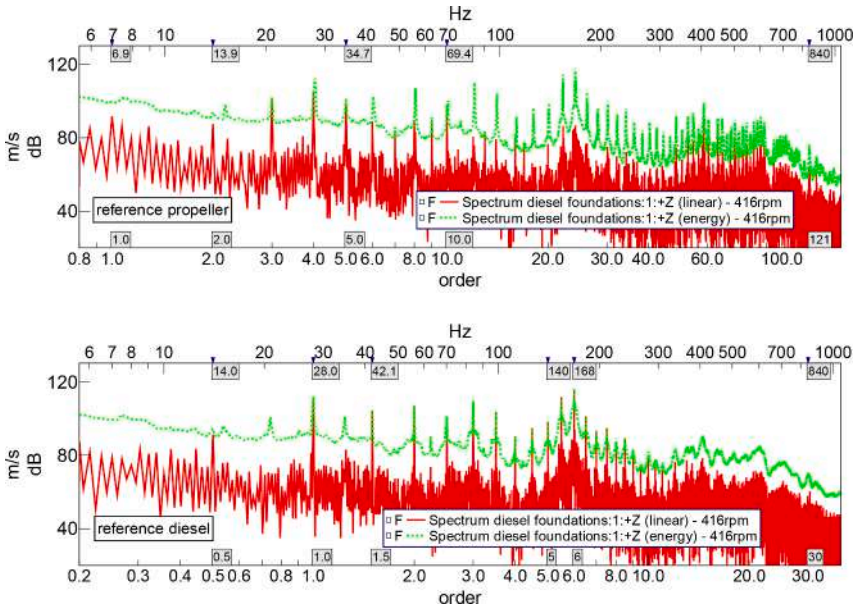


**Fig. 4.** $n_{prop}$ = 416 rpm - 17knots – $J$ = 0.783 - narrow band energy and linear synchronously averaged vibration spectra on the diesel engine foundation at the diesel engine foundations in correspondence of one of the resilient mounts (top: reference propeller, bottom: reference diesel).

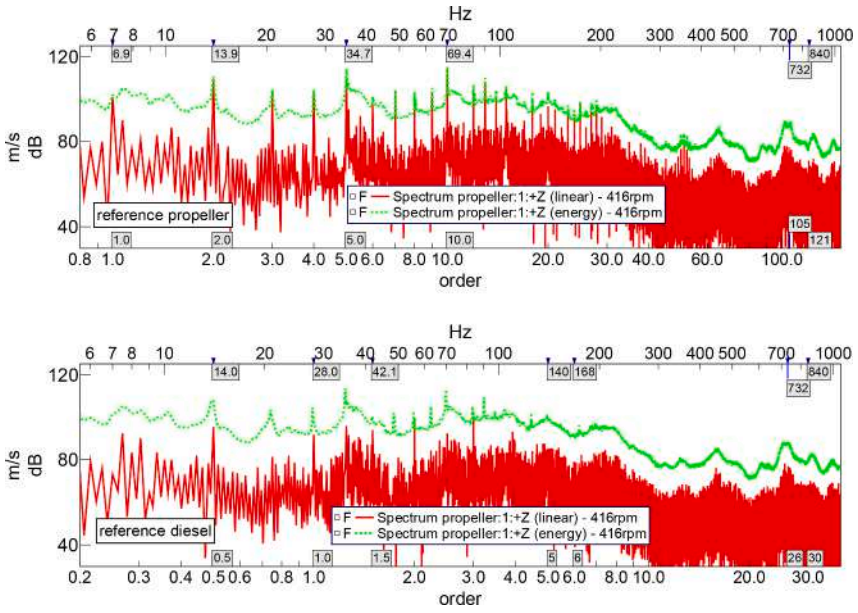


**Fig. 5.** $n_{prop}$ = 416 rpm - 17knots - $J$ = 0.783 - narrow band energy and linear synchronously averaged vibration spectra on the hull shell immediately above a propeller (top: reference propeller, bottom: reference diesel).

crankshaft rotation (1X) and combustion (6X) as in the 12 cylinder 4 stroke engine, there are six bursts per cycle corresponding to excitation by the explosions taking place in each cylinder. Propeller harmonic is not evident. On the contrary adopting as reference the propeller rotation, the obtained linear synchronously averaged spectrum is characterized by propeller revolution frequency (1X order) related to residual mechanical unbalance. Moreover, 2X order and higher multiples components can be well identified. The propeller blade passage content is also detectable which is equivalent to 5X order. The adopted frequency resolution (depending on time history length and the number of samples for average computation) make the presence of peaks at similar frequency related to two distinct harmonic content (e.g. propeller shaft rotation and second order of the engine crankshaft rotation).

The harmonic content related to diesel engine excitation is higher than the one related to the propeller which however is not negligible to underline the presence of a structural coupling between engine foundation and propeller shaft line through bearing axial forces. A significant energy content at the gear mesh frequency of the gearbox is also detectable (order 121X and 30X if reference respectively to the propeller or diesel engine shaft).

Energy synchronously averaged vibration spectra is characterized by significant high frequency contents probably related to a more random nature of system response probably related to the presence of repetitive bursts due to engine combustions and possible propeller cavitation phenomena able to excite high frequency system structural resonances.

Analogous results analysing the averaged complex spectra evaluated on the hull shell immediately above a propeller at propeller shaft 416 rpm (Fig. 5). The harmonic content related to propeller excitation is higher than the one related to the diesel engine. However also in this case both are not negligible.

The energy average spectrum shows power continuously distributed in the whole frequency domain, thus indicating they are essentially random in nature in the system response measured on the hull shell above a propeller. The high frequency peak a 732 Hz may be related to a system resonance exited by impulsive phenomena associated to propeller cavitation and other burst sources. This will be more evident in the vibration response time frequency analysis during propeller rotational speed run up reported in the following. Significant high distributed power in the frequency range 45–250 Hz is also detectable in the energy spectrum may be related also in this case to burst anomalous phenomena acting on the system as propeller cavitation.

Fig. 6 shows the linear synchronously averaged vibrational spectra referred to engine and propeller measured at the main deck where the passenger areas are located for the previous considered propeller rotational speed. Spectra contents are lower than the previous points especially at high frequency values and the vibration reduction is related to the use of viscoelastic materials coupled with the main steel structure generating good level of isolation (Silvestri et al., 2021). However, gear mesh frequency content is well detectable even if characterized by a low energy level.

Fig. 7 compares narrow band energy averaged vibration spectra measured on the hull shell immediately above a propeller at two propeller rotational speeds corresponding to two ship velocities. The spectra are displayed using both propeller order (top) and derived frequency (bottom) for the x-axis representation. Main propeller orders generally exhibit higher energy levels at the higher rotational speed. Invariant frequencies contents can also be detectable (see cursors at 732 Hz and 1653 Hz).

The rms values are computed on the whole acquisition frequency band of the linear synchronous averaged spectra referring both to the diesel and propeller source at main, upper and sun deck for two propeller rotational speeds. The obtained values are representative of the energy harmonic content of the system response associated with each source. The rms value evaluated on the averaged energy spectrum provide the global contribution that includes the harmonic contributions of all sources acting on the system including the random nature ones. Propeller contribution is in general higher than the engine one at higher rotational speed. The rms value is also computed on the acoustic response measured near the swimming pool. Comparison results are reported in Fig. 8.

The variance spectra were computed on the synchronous linear vibrational spectra at four propeller rotational speeds. In Fig. 9, the variance frequency contents associated with the blade passage component and its second order (5X and 10X) are reported adopting logarithmic scale. It is observed that the variance evaluated on specific components of the spectrum showing good sensitivity approaching propeller cavitation region. At 268 rpm and 330 rpm cavitation is supposed not present and variance value in correspondence of the blade passage content and its second order content is negligeable. On the contrary, the previous frequency components are significant at the two

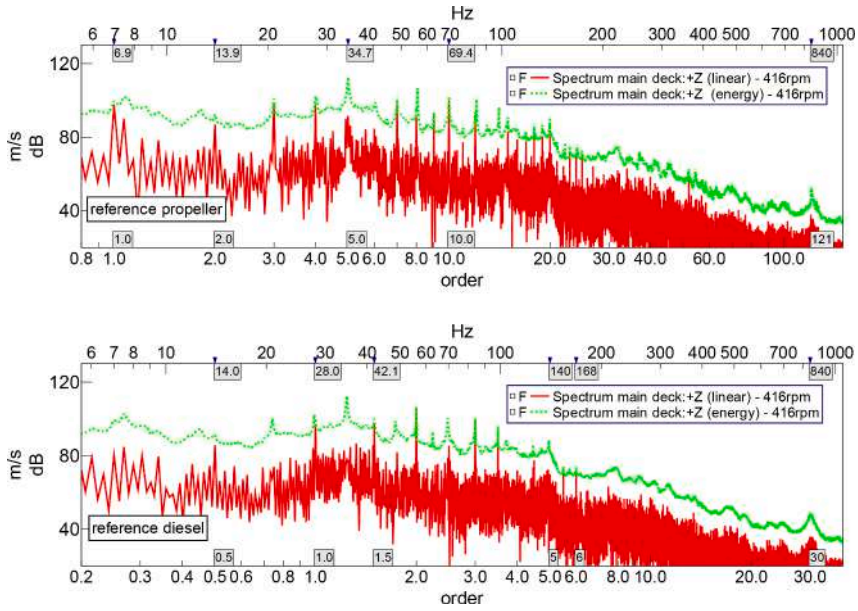


**Fig. 6.** $n_{prop}$= 416 rpm - 17knots - $J = 0.783$ - narrow band energy and linear synchronously averaged vibration spectra on the main deck (top: reference propeller, bottom: reference diesel).

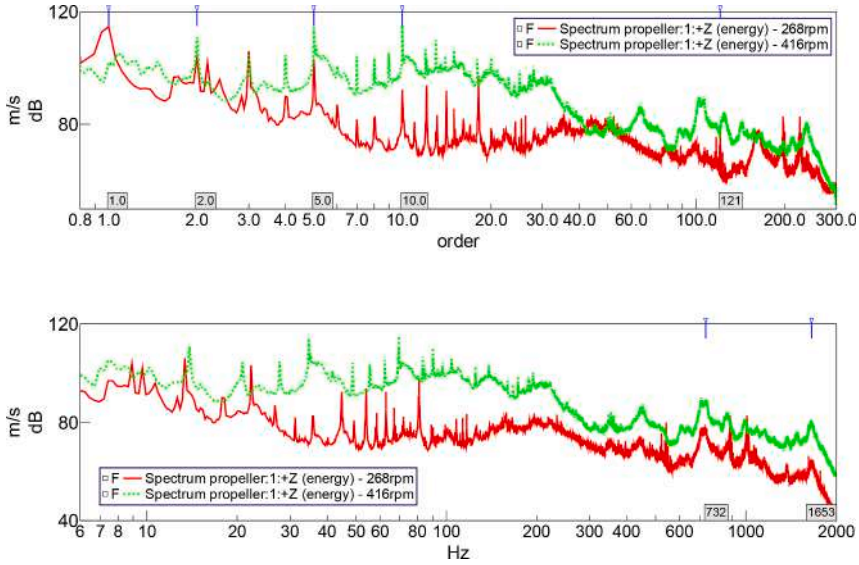


**Fig. 7.** $n_{prop}$= Narrow band energy averaged vibration spectra on the hull shell immediately above a propeller at two propeller rotational speeds: 268 rpm (11knots) – $J = 0.784$ and 416 rpm (16knots) – $J = 0.783$.

higher propeller rotational speeds to indicate the rise of random energy contribution in the signal may be related to a diffused vorticity of propeller and turbulent phenomena.

The high level of variance at 416 rpm and 434 rpm seem to clearly indicate the blade passage phenomenon is more random in its nature may be related to a burst content in its periodic pattern attributable to a phenomenon to cavitation inception.

The Fig. 10 shows the overall level of the measured vibration on the hull shell above a propeller during a speed run-up test ranging from 221 rpm to 416 rpm.

During the transient, at low rotational speeds the vibration level slowly increases while an evident and sudden climbing trend is well detectable when the propeller rotational speed reaches 326 rpm.

This seems to suggest the rise of an anomalous condition that occurs suddenly and which may be related to the inception of burst phenomena such as cavitation bubbles and the consequent onset of cavitation in the propeller adding significant energy to vibrational response in addition to wake contributions.

Crossing the threshold value of rotational speed the cavitation become intense and the vibration overall value increases further. This behaviour is in a good agreement with the cavitation evolution model in (Vergassola, 2019; Kalikatzarakis et al., 2022) and therefore seems to justify the presence in the investigated superyacht of an operating range at higher propeller rotational speeds where propeller cavitation is completely developed.

Fig. 11 shows the time-frequency analysis of the vibration response measured on the hull shell above a propeller during speed run up, obtained by Short Time Fourier Transform (STFT). Results evidence that in low frequency range, the component related to the blade passage phenomenon and higher multiples are evident (see oblique cursers). In addition the diesel engines half order (engine cycle) is significant.

Invariant high frequency contents (see vertical cursors at 732 Hz and

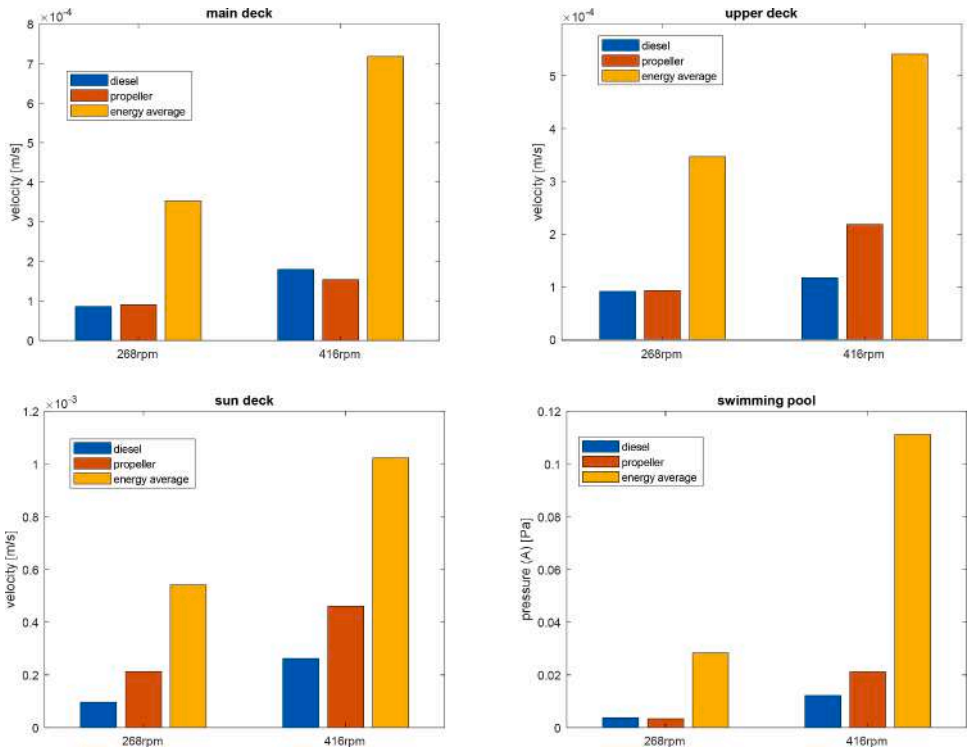


**Fig. 8.** Propeller, diesel engine and overall contributions to the target for two propeller rotational speeds (268 rpm -> 11knots and 416 rpm -> 17knots).

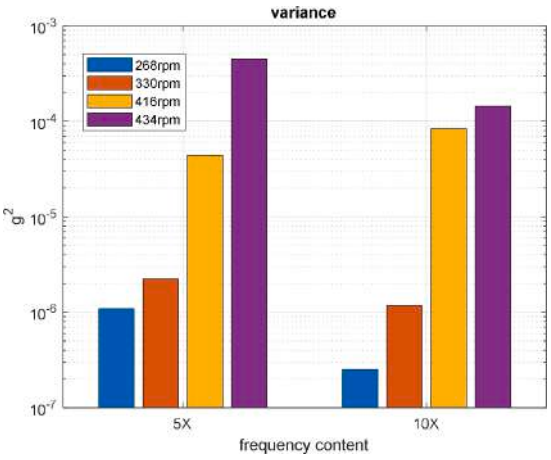


**Fig. 9.** Variance blade pass components calculated on the vibration signal on the hull shell immediately above a propeller for 4 propeller rotational speeds (268 rpm -> 11knots, 330 rpm -> 15knots, 416 rpm -> 17knots, 434 rpm -> 18knots).

1653 Hz) become apparent above the previous identified threshold propeller rotation speed 326 rpm in the overall level analysis. This behaviour seems also to confirm above a specific propeller rotational speed the onset of an anomalous burst phenomenon exciting structural resonance may be related to cavitation.

Further evidence of the possible presence of cavitation at the maximum speed can be found in Fig. 12, where the Burrill cavitation diagram is reported, where the working area of the propeller at 416 rpm is shown in red.

As it can be seen from the Fig. 12, it is highly probable that at least the 10 % of back cavitation is probable, while the working area is below the maximum limit proposed by Blount in (Blount and Bartee, 1997) for highly loaded propeller. Moreover, the clearance between the tip of the propeller and the hull is lower than 18 % of the propeller diameter, allowing an important propagation of induced acceleration to the vessel.

### 4.2. *Spectral kurtosis and demodulation analysis results*

Vibrational response signals have been considered for the detection of incipient propeller cavitation using SK, and the kurtogram has been employed for subsequent envelope analysis.

Fig. 13 illustrates the computation of the Fast-Kurtogram using Antoni's algorithm (Antoni, 2006), evaluated on the vibration signal measured on the hull at the propeller constant rotational high speed of 418 rpm, where cavitation phenomenon occurs. By examining the colormap, it is possible to identify frequency bands with abnormally high values, indicating the potential presence of maximum impulsivity of a signal related to an anomalous phenomenon acting on the system. The kurtogram reveals significant high values at a central frequency of 1650 Hz at level 5.5, corresponding to a bandwidth of 45 Hz. This frequency band exhibits the highest signal-to-noise ratio, making it optimal for demodulating the signal using this bandpass filter and at the same time preserving the impulse-like nature.

The method seems to successfully identify an optimal detection bandpass filter centred on a specific frequency band more sensitive to onset of cavitation, indicating the onset of an anomalous condition related to this phenomenon. The central frequency is related to a system structural resonance well excited by the cavitation exciting loads. It is worth noting that the recognized frequency ranges from SK are not precisely identical to those obtained from the signature analysis, as the dyadic filter bank approach employed in the Fast Kurtogram has some limitations in spectral resolution. Different propeller rotational speed conditions have been considered, filtering the acquired vibrational signal data on the hull near propeller within the frequency band previously identified by kurtogram and spectral kurtosis results at 416 rpm. Subsequently, envelope spectrum analysis is conducted on the filtered signal to identify the presence of modulation phenomena. In this way the demodulation process was kept constantly amongst the different tests.

At propeller rotational speed equal to 268 rpm and 330 rpm, as shown in Fig. 13 (top and central up), no diagnostic frequency

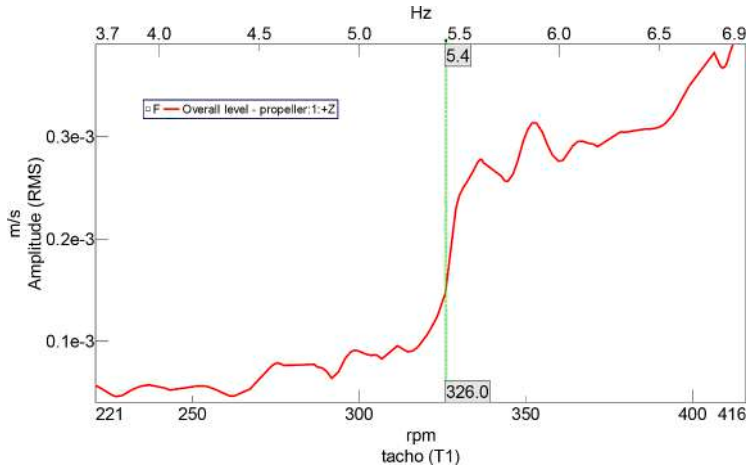


**Fig. 10.** Vibrational overall level for the accelerometer signal on the hull shell above a propeller during speed run up.

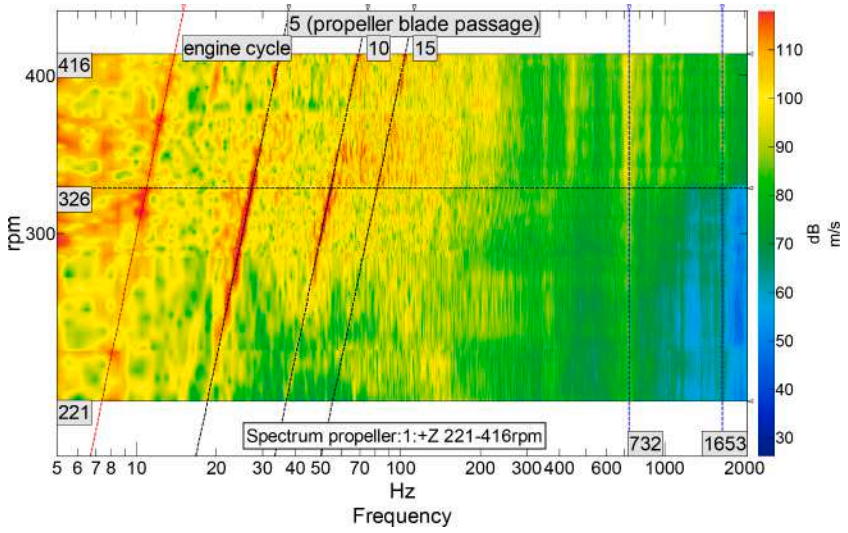


**Fig. 11.** STFT for the accelerometer signal on the hull shell above a propeller during speed run up.

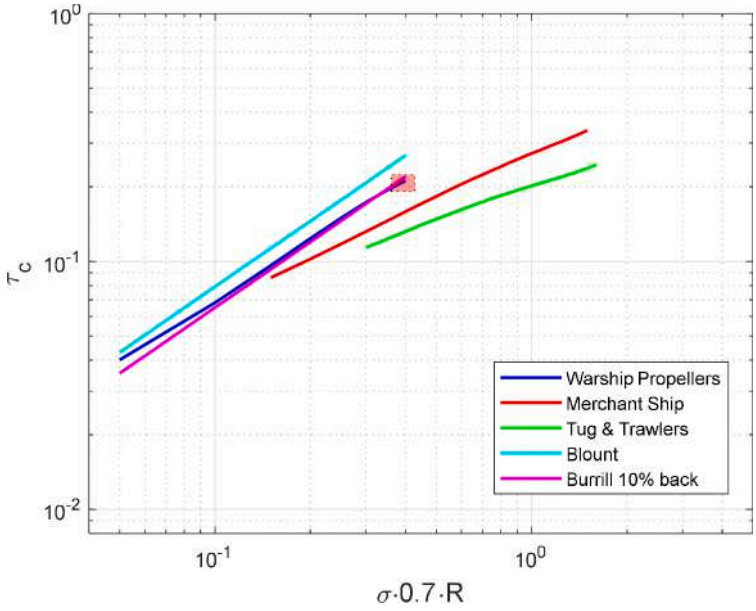


**Fig. 12.** Burrill cavitation diagram; the working area at np=416 rpm is highlighted in red.

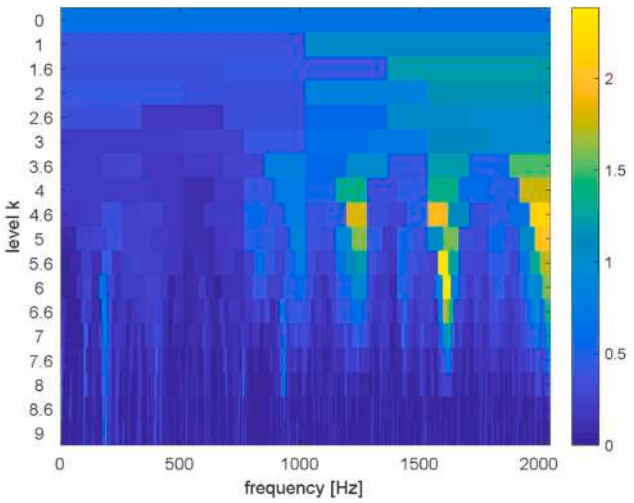


**Fig. 13.** Fast-kurtogram for the vibrational signal at 416 rpm measured on the hull shell immediately above a propeller.

component related to propeller rotation is detectable in the squared envelope spectra, implying no cavitation on the propeller blade.

Differently, from Fig. 14 (central down and bottom), it is evident that a low-frequency content and consecutive harmonic components related to the shaft propeller rotational frequency rise strongly as the system increases its rotational speed and cavitation rises in an increasingly significant way.

As stated above, the key idea of demodulation process supported by spectral kurtosis analysis is to identify the repeating frequency of impact-like signal, not considering the whole frequency contents of the raw signal, but a restrict frequency band of the maximum SK. This allows to eliminate not only low frequency components that are common in rotating machinery including shaft misalignment, unbalance, but also other noises that are not directly related with propeller cavitation.

When cavitation conditions are reached, the propeller rotational frequency and higher multipliers dominate the envelope spectrum shown in Fig. 14 (central down and bottom). On the contrary, the envelope spectrum evaluated far from cavitation conditions reported in Fig. 14 (top and central up) shows no diagnostic frequency component, implying no anomalous phenomena acting on the propeller. According to the obtained results, in cavitation condition, related frequency contents measured in dynamic responses are modulated by shaft rotation constant low repeating frequency.

This put in evidence the presence of a frequency content in the measured response whose origin is strictly relate to propeller operation.

Cavitation phenomenon seems to contribute to excite a system structural resonance whose energy trend in the measured system response is conditioned by the cavitation impulsive nature (Lee and Seo, 2013).

It is worth mentioning the results obtained with the proposed method are conditioned by the optimal bandpass-filter design identified by SK. If a non-optimum filter is adopted, the resulting envelope spectra would show no diagnostic frequency component distinctively.

The proposed procedure appears capable of identifying, in the system's dynamic response when incipient cavitation occurs, the emergence of specific weak diagnostic contents in the vibration signal not easily identifiable with a classical FFT analysis.

In the present activity, differently from (Lee and Seo, 2013) where the method based on SK has been applied on hydrophone output signals, vibrational responses have been considered. This has allowed to verify the good diagnostic capability of the method also using structural responses by collecting operational signal from accelerometers properly positioned on the hull.

The reliability of the technique with vibrational responses allows the use of experimentally tested, cost-effective solutions to predict and diagnose the anomalous condition of cavitation approaching, using non-intrusive sensors such as accelerometers.

The method considered high frequency contents related to structural resonances exited by cavitation phenomenon and these ranges seems to be good for accelerometers measures. The obtained reliable diagnostic results, even using structural response, can be attributed to the high signal-to-noise ratio values of the accelerometer in the high-frequency range. This allows for the accurate monitoring of high-frequency fluid dynamic phenomena and, consequently, the correct detection of the rise of anomalous transients involving blade passage and propeller rotation.

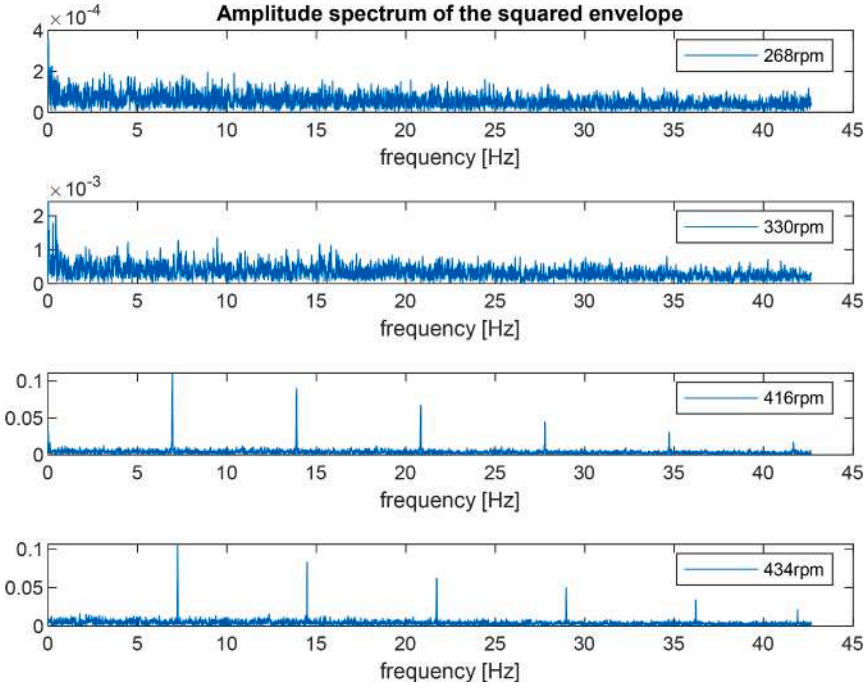


**Fig. 14.** Amplitude spectrum of the squared envelope for not (top and central up) and cavitating (central down and bottom) conditions.

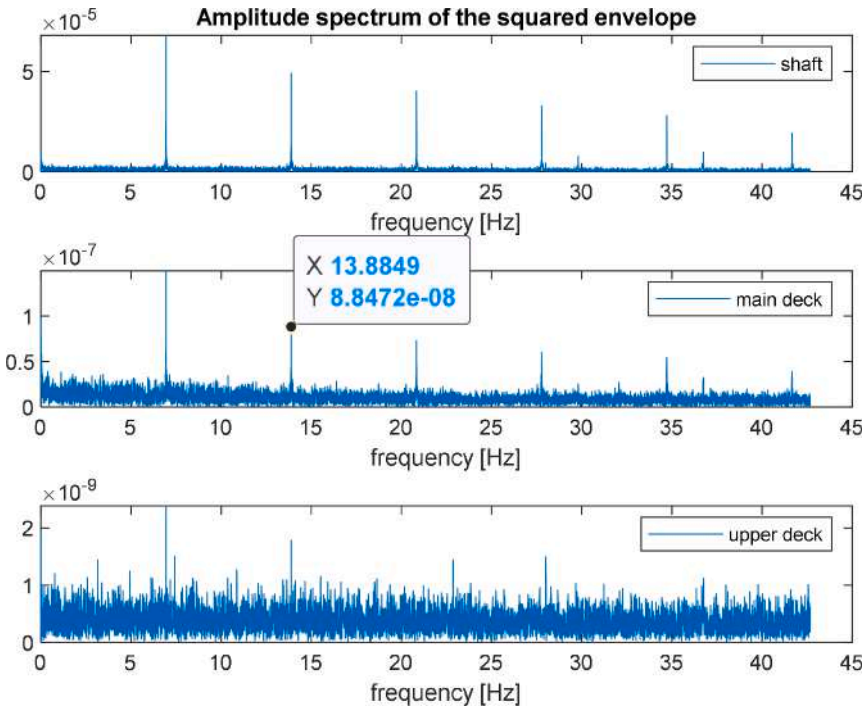


**Fig. 15.** Amplitude spectrum of the squared envelope at propeller rotational speed 416 rpm: the propeller shaft is the fundamental component ($1X_{proppeler} = 6.93$ Hz; $2X_{proppeler} = 13.88$ Hz $\neq 0.5X_{diesel} = 14.00$ Hz, see data cursors in the figure).

Similar results were obtained by applying the procedure considering different dynamic response measurement points. In Fig. 15, the envelope spectrum is calculated on the propeller shaft lubricated bearing on the hull and on two decks (main and upper) in the previously considered condition at 416 rpm where cavitation occurs. The central frequency and bandwidth values identified with the method are the same as in the previous case where the signal measured on the hull near propeller. The extracted modulation frequency in all considered response points is always the same corresponding to the propeller shaft rotation. The modulating effect is less marked in the case of the upper deck, probably for the presence of isolation materials able to reduce vibrational energy propagation at the higher frequency values.

The method has been applied using vibrational responses acquired both on the engine foundation and on the engine block. In addition, in this case the signals were filtered in the previous identified frequency band for the subsequent frequency analysis on the filtered signal Hilbert envelope.

Results are reported in Fig. 16 for 416 rpm propellers rotational speed.

Different from the previous cases, the demodulation process indicates the high frequency content related to system resonance is modulated by engine characteristic frequencies (engine cycle at 14.00 Hz) and not significantly by propeller shaft rotation (due to the gearbox with transmission ratio equal 4.03, $1X_{proppeler} = 6.93$ Hz and $2X_{proppeler}$ 13.88 Hz $\cong$ $0.5X_{engine} = 14.00$ Hz = engine cycle frequency, see cursors in Figs. 15 and 16).

The demodulation process has been also applied on the diesel foundation vibrational response at a low propeller rotational speed where cavitation phenomenon is supposed doesn't occurs.

The competed amplitude spectrum of the squared envelope reported in Fig. 17 shows also in this case that the burst energy, related to engine combustion is able to excite the previous system resonance (corresponding to the central frequency of the band pass filter) and this energy content is modulated by the periodicity of the cycle.

This seem to indicate how the measured responses on the diesel block and foundation are always affected by a modulation phenomenon involving the previous resonance also when cavitation doesn't occur. In this case the related content mainly exited by the combustion burst engine excitation and diesel operation and not the contents related to the cavitation excitation. This is confirmed by the presence of the phenomenon at all operation speed including the lower ones.

The identified components on the envelope spectrum, although very close in frequency to those of propeller rotation and higher multiples, are distinct from these to indicate how energy signal content related to the exited resonance is modulated by the diesel engine and not by the propeller.

The obtained results seem to indicate that dynamic response energy evaluated in the frequency band indicated in the kurtogram is mainly related to the source largely conditioning the considered response point and this seems to justify the identification of distinct periodicity (shaft propeller or diesel cycle) in the envelope spectrum in the previous cases (Fig. 18).

Coherent results were obtained also using a microphone signal at the upper desk near swimming pool. External noise detected by the microphone made the identification less evident applying the methods. In this case the demodulation has been done non-considering the previous structural resonance frequency, but a lower value related to an acoustic propeller emission frequency content in cavitation.

### 4.3. Cyclostationarity results

The cyclostationarity analysis has been applied on the operational vibration responses and cyclic spectral density function has been computed on vibration response measured on the hull shell above a propeller for operating conditions characterized by different propeller rotational speeds.

To show results, a colormap representation is adopted where the modulating frequencies are in the axis of the abscissas (α cyclic frequency) while spectrum frequencies are in the axis of the ordinates (bi-frequency plan) (Antoni, 2009; Antoni and Hanson, 2012). In the maps spectrum frequency range is extended to the whole frequency acquisition band while cyclic frequency range is limited up to the first multipliers of the propeller blades frequency content (0–60 Hz).

The aim is to investigate propeller blades frequency interactions with

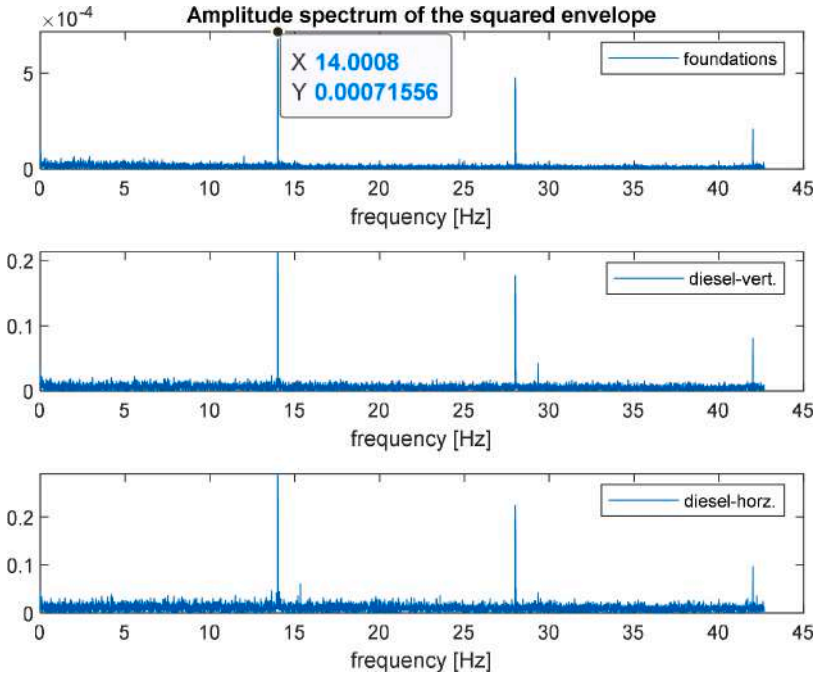


**Fig. 16.** Amplitude spectrum of the squared envelope at propeller rotational speed 416 rpm: the engine cycle $0.5X_{engine}$ is the fundamental component (14.00 Hz).

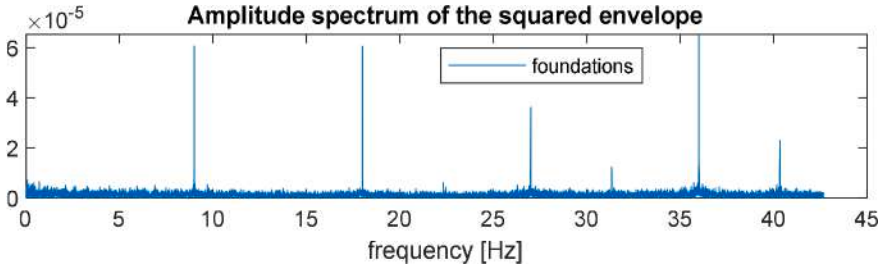


**Fig. 17.** Amplitude spectrum of the squared envelope at propeller rotational speed 268 rpm: the engine cycle 0.5X is the fundamental component (8.9 Hz).

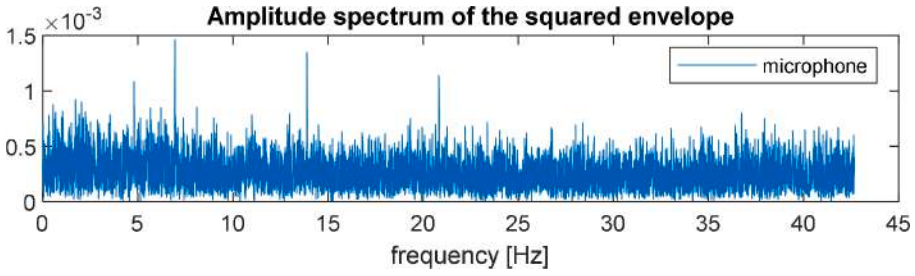


**Fig. 18.** Amplitude spectrum of the squared envelope at propeller rotational speed 416 rpm: the propeller shaft is the fundamental component.

broad band high frequency modulations phenomena may rise in cavitation condition and how they modify their energy varying propeller rotational speed.

Fig. 18 shows the cyclic spectral density computation at 416 rpm where cavitation phenomenon is supposed to have been established.

The energy contents distributed near $\alpha = 0$ are related to stationary data: it is possible to detect response contributions 732 Hz, 1650 Hz, corresponding to possible system resonances excited by propeller cavitation. Moreover, a low frequency content around 70 Hz already identified in the operational spectra in Fig. 5 related to a second multiplier of propeller blade frequency.

On the other hand, the energy contents distributed in correspondence of $\alpha \neq 0$ values are linked to non-stationary contributions which consists of amplitude modulated signal components characterized by a cyclic modulation.

A marked point at the cyclic frequency $\alpha = 34.7$ Hz and a double value of spectral frequency indicates an interaction between the first and second multiple of the propeller blade.

The colormap is characterized by a number of high energy distinct points well detectable on the spectral frequency axis f at 732 Hz and 1650 Hz, which may correspond to the previous detected values of possible system resonances excited by propeller cavitation. The spacing of the points is 34.6 Hz in the horizontal direction and this seems to indicate the presence of cyclostationarity related to a modulation effect by the propeller shaft frequency on these high frequency contents.

The distribution of energy along the spectral frequency contents at 732 Hz and 1650 Hz it is not only made up of marked points along the cyclic frequency $\alpha$ at the propeller shaft rotation and higher multiplier

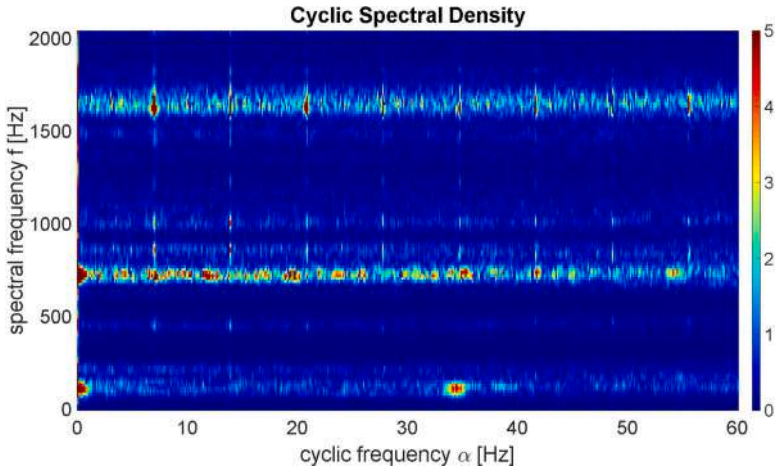


**Fig. 19.** Cyclic spectral density of the vibrational response measured on the hull above a propeller - $n = 416$ rpm - cavitation (cyclic frequency range 0–60 Hz).

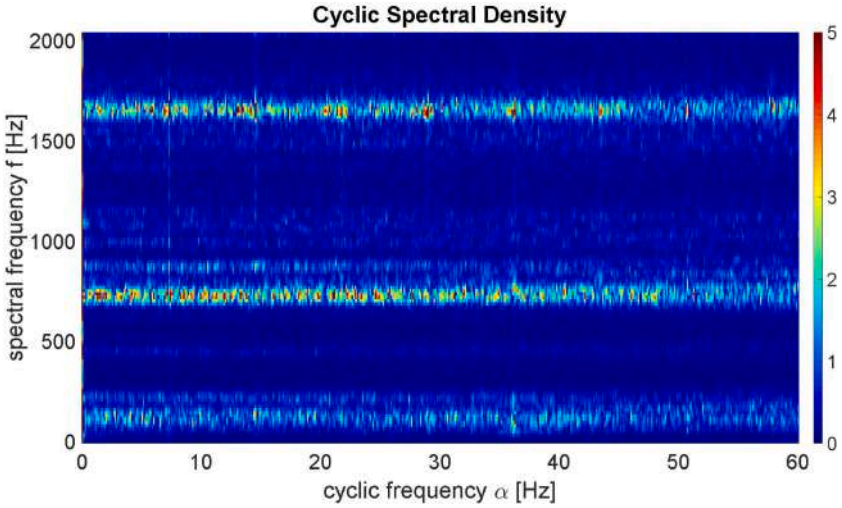


**Fig. 20.** Cyclic spectral density of the vibrational response measured on the hull above a propeller - n =434rpm - cavitation (cyclic frequency range 0-60Hz)

(including propeller blade pass frequency), but also of a continuous distribution of energy. This reveals that these energy contents are actually periodic in their waveform (system resonance response contents) with additional random contributions.

The two excited resonances at 732 Hz and 1650 Hz seem to be mainly synchronized on propeller shaft rotation and higher multiplier and random contribution may rise approaching cavitation conditions.

By observing the map in Fig. 19 at fixed values of α cyclic frequency it possible to note significant peaks clearly discernible around 35 Hz on the previous detected spectral lines. This seems to indicate what has already emerged from previous analyses that the vibration energy around 700 Hz and 1650 Hz (related a possible resonances well excited by cavitation phenomenon) is modulated by a spectral content with characteristic frequency at 35 Hz related to propeller rotation. In such conditions, the previous high frequency contents seem to modulate the propeller blades frequency in a marked way.

Significant values in the cyclostationary energy at the cyclic frequencies related shaft rotation was also detected at a higher propeller rotational speed (434 rpm, see Fig. 20).

In addition, in this case cyclostationarity results seems to indicate a periodic modulation related to propeller rotation on the previous detected high frequency carrier related to structural resonance exited by cavitation phenomenon. An additional spectral frequency around a 180 Hz is also detectable also this related to an excited system resonance.

It is important also to mention that these cyclic spectral components are not present in a marked way in the cyclic spectral density when it was computed on a vibrational response at a lower propeller rotational speed (see Fig. 21).

The low values of these contents in the cyclostationary energy may justified by a not marked excitation of the previous system resonances at low propeller rotational speed due to the absence of the cavitation phenomenon. However, the non-zero values seem to indicate a “link” between system resonances (180 Hz, 732 Hz, 1650 Hz) excited by other dynamic phenomena acting on the system and the propeller blade pass frequency well detectable by cyclostationary analysis.

However, in the cyclic spectral density map these contributions are well distinguishable and this seems to prove how cyclic spectral density can detect phenomena from a weak signal also in presence of background noise (Antoni, 2009).

The obtained results seem to indicate as cyclostationary analysis can provide an effective tool for proper identification and the correlation of the several modulation mechanisms present in the signal and so it seems fine for cavitation identification.

## 5. Conclusions

The forced vibration analysis presented in this paper provides a more comprehensive experimental characterization of superyachts vibrational behaviour in different operational conditions.

At first, a signature investigation is presented in terms of vibrational

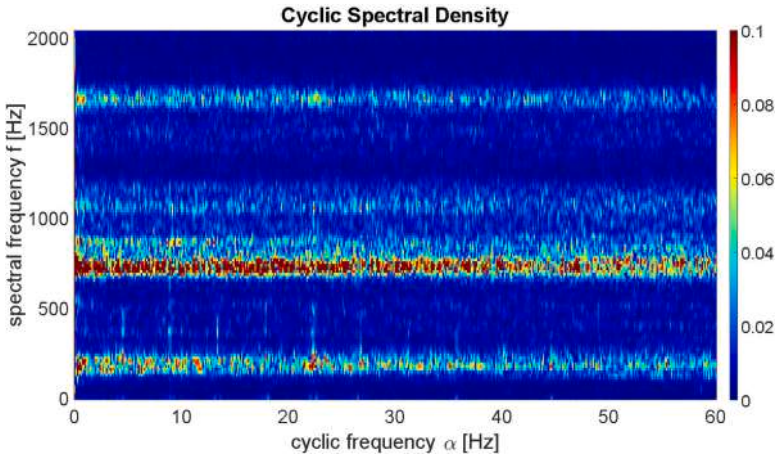


**Fig. 21.** Cyclic spectral density of the vibrational response measured on the hull above a propeller - $n = 268$ rpm - no cavitation (cyclic frequency range 0–60 Hz).

response analysis and source contribution to vibrational targets on the vessel. This preliminary analysis provided a detailed system identification at low propeller rotational speed far from cavitation and at higher values where cavitation may rise. Synchronous linear averages were performed on complex operational spectra and allowed to obtain information about deterministic components while energy average allows to put in evidence the power continuously distributed in the whole frequency domain and so to detect the rise of random energy contents approaching a cavitation condition. At high propeller speed, modulation phenomena were also identified, which may be ascribable to an interaction between propeller rotation and the yacht structure, since structural resonances excited by the onset of cavitation and wake phenomena was observed. Spectral variance computation seems to be attractive for cavitation detection as it is characterized by short computation times and therefore suitable for real-time diagnostics application. The herein proposed methodology allow the usage of experimental full scale vibrational analyses for identifying pure hydrodynamic sources, such as cavitation and wake, that are cheaper and easier to be carried out instead of complex underwater measurement campaign. The instrumental set up of such full-scale measurements can be selected by applying spectral kurtosis, selecting the optimal filter design for demodulation of system responses for cavitation detection.

The diagnostic capability of cyclic spectral density function was also assessed in this research, for detecting the rise of cavitation condition. The cyclic spectral density function allows to indicate a strict connection between the presence of modulation phenomena and the arise of propeller cavitation at higher rotational speed. Indeed, cyclic spectral density function seems to be an appropriate tool to detect as propeller shaft rotation contents and its higher multiplier are influenced by moving towards cavitation conditions.

The diagnostic methods herein tested may be included in an innovative reliable control system which is able to prevent cavitation risks using cheap not intrusive vibrational sensors.

## CRediT authorship contribution statement

**Paolo Silvestri:** Writing – original draft, Methodology, Investigation, Data curation, Conceptualization. **Tatiana Pais:** Writing – original draft, Supervision, Methodology, Investigation, Data curation, Conceptualization. **Gianmarco Vergassola:** Writing – original draft, Validation, Methodology, Investigation, Formal analysis, Data curation, Conceptualization.

## Declaration of competing interest

The authors declare that they have no known competing financial interests or personal relationships that could have appeared to influence the work reported in this paper.

## Data availability

No data was used for the research described in the article.

## References

Aktas, B., Atlar, M., Turkmen, S., Shi, W., Sampson, R., Korkut, E., Fitzsimmons, P., 2016. Propeller cavitation noise investigations of a research vessel using medium size cavitation tunnel tests and full-scale trials. Ocean Eng. 120, 122–135.

American Bureau of Shipping, 2006. Guidance Notes on Ship Vibration.

Antoni, J., Hanson, D., 2012. Detection of surface ships from interception of cyclostationary signature with the cyclic modulation coherence. IEEE J. Oceanic Eng. 37 (3), 478–493.

Antoni, J., Randall, R.B., 2006. The spectral kurtosis: application to the vibratory surveillance and diagnostics of rotating machines. Mech. Syst. Signal Process. 20, 308–331.

Antoni, J., 2006. The spectral kurtosis: a useful tool for characterizing nonstationary signals. Mech. Syst. Signal Process. 20, 282–307.

Antoni, J., 2009. Cyclostationarity by examples. Mech. Syst. Signal Process. 23, 987–1036.

Asmussen, I., Menzel, W., Mumm, H., 2001. GL-Technology: Ship vibrations. Germanischer Lloyd.

Bassetti, M., Gaggero, F., Prato, A., Schiavi, A., Pais, T., Silvestri, P., Lembo, E., 2022a. Assessment of shipboard sound insulation in the low frequency range through a laboratory experimental methodology based on a modal approach. Progress in Marine Sci. Technol. 6, 374–381. https://doi.org/10.3233/PMST220045.

Bassetti, M., Tonna, R., Pais, T., Silvestri, P., Lembo, E., Iuliano, A., 2022b. Application of transfer path analysis technique to cruise ships. Progress in Marine Sci. Technol. 6, 397–407. https://doi.org/10.3233/PMST220047.

Biot, M., De Lorenzo, F., 2007. Open issues regarding noise and vibrations on board cruise ships: a suggested approach for measuring comfort. In: Proceedings of the "Autumn Conference 2007: Advanced in Noise and Vibration Engineering. Institute of Acoustics, Oxford, UK, pp. 17–18. October.

Blount, D.L., Bartee, R.J., 1997. Design of propulsion system for high speed craft. Mar. Technol. 34 (4), 276–292. Oct.

Borelli, D., Gaggero, T., Rizzuto, E., Schenone, C., 2021. Onboard ship noise: acoustic comfort in cabins. Applied Acoustics 177 (107912) art.

Braun, S., 2011. The synchronous (time domain) average revisited. Mech. Syst. Signal. Process 25 (4). https://doi.org/10.1016/j.ymssp.2010.07.016. ISSN 0888-3270.

Combet, L., Gelman, L., 2007. An automated methodology for performing time synchronous averaging of a gearbox signal without speed sensor. Mech. Syst. Signal. Process 21 (6), 2590–2606.

Fyfe, K.R., Munck, E.D.S., 1997. Analysis of computed order tracking. Mech. Syst. Signal. Process 11 (2), 187–205. https://doi.org/10.1006/mssp.1996.0056.

Kalikatzarakis, M., Coraddu, A., Atlar, M., Gaggero, S., Tani, G., Villa, D., Oneto, L, 2022. Computational prediction of underwater radiated noise of cavitating marine propellers: on the accuracy of semi-empirical models. Ocean Eng. (111477), 259. , art.

Lee, Jeung-Hoon, Seo, Jong-Soo, 2013. Application of spectral kurtosis to the detection of tip vortex cavitation noise in marine propeller. Mech. Syst. Signal. Process 40 (1), 222–236. ISSN 0888-3270.

Lloyd's Register, 2006. Ship Vibration and Noise - Guidance Notes", Revision 2.1.

McFadden, P.D., Toozhy, M., 2000. Application of synchronous averaging to vibration monitoring of rolling element bearing. Mech. Syst. Signals Process. 14, 891–906.

Oppenheim, A.V., Schafer, R.W., 1999. Discrete-time Signal Processing. Prentice-Hall, Inc., Upper Saddle River, NJ, USA.

Prato, A., Silvestri, P., Pais, T., Gaggero, F., Schiavi, A., 2023. Airborne sound transmission loss of ship bulkheads: a new methodological approach for in-laboratory assessment by including low frequencies. Ocean Eng. (115428), 285. https://doi.org/10.1016/j.oceaneng.2023.115428. , art.

Silvestri, P., Pais, T., Gaggero, F., Bassetti, M., 2021. Dynamic characterization of steel decks with damping material by impact test. Int. J. Struct. Stab. Dyn. 21 (7) https://doi.org/10.1142/S0219455421500966 art. no. 2150096.

Vergassola, G., 2019. The prediction of noise propagation onboard pleasure crafts in the early design stage. J. Ocean Eng. Mar. Energy,. https://doi.org/10.1007/s40722-019-00149-4.